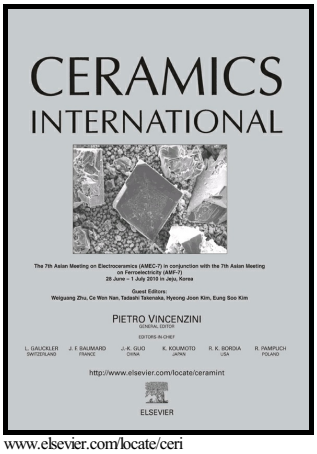

www.elsevier.com/locate/ceri

Fine zircon ($ZrSiO_4$) powder mechanical activation, a Perturbed Angular Correlation (PAC) analysis

Matías R. Gauna, Nicolás M. Rendtorff, María S. Conconi, Gustavo Suárez, Alberto Pasquevich, Patricia C. Rivas, Laura Damonte

PII: S0272-8842(17)31243-9
DOI: http://dx.doi.org/10.1016/j.ceramint.2017.06.041
Reference: CERI15563

To appear in: *Ceramics International*

Received date: 11 February 2017
Revised date: 2 May 2017
Accepted date: 6 June 2017

Cite this article as: Matías R. Gauna, Nicolás M. Rendtorff, María S. Conconi Gustavo Suárez, Alberto Pasquevich, Patricia C. Rivas and Laura Damonte, Fin zircon ($ZrSiO_4$) powder mechanical activation, a Perturbed Angular Correlatio (PAC) analysis, *Ceramics Internationa* http://dx.doi.org/10.1016/j.ceramint.2017.06.041

Fine zircon ($ZrSiO_4$) powder mechanical activation, a Perturbed Angular Correlation (PAC) analysis

Matías R. Gauna[1], Nicolás M. Rendtorff[1,2*], María S. Conconi[1], Gustavo Suárez[1,2], Alberto Pasquevich[3], Patricia C. Rivas[3,4], Laura Damonte[3]

[1]Centro de Tecnología de Recursos Minerales y Cerámica (CETMIC): (CIC-CONICET-CCT La Plata) Argentina. Camino Centenario y 506. C.C.49 (B1897ZCA) M.B. Gonnet. Buenos Aires, Argentina.

[2]Departamento de Química, Facultad de Ciencias Exactas - UNLP, Argentina.

[3]Departamento de Física, IFLP, Facultad de Ciencias Exactas, UNLP, La Plata, Argentina.

[4]Facultad de Ciencias Agrarias y Forestales, UNLP, La Plata, Argentina.

[*]Corresponding author: Tel.: +542214840247/ Fax: +542214710075. rendtorff@cetmic.unlp.edu.ar

Abstract

By means of Perturbed Angular Correlation (PAC) analysis the resulting phases during mechano-chemical activation process on zircon ($ZrSiO_4$) commercial fine powder ($D_{50}\cong 0.8$ µm) were accurately identified and characterized.

A high energy planetary mill was employed with 850 rpm up to 120 minutes. The phenomenological macroscopic confirmation of the structural change and mechanical activation consisted in an important enhancement of the sintering behavior of the treated fine zircon powders.

Three different well known zircon phases were identified and quantified as a function of the milling time: a fully crystalline phase, an aperiodic phase and a distorted phase. A

decrease in the first two phases was accompanied by the appearance of the third one; finally, at long term treatments, a partial dissociation was observed. Particularly the resulting zirconium oxide is a highly distorted one. The results were discussed together with those obtained using XRD, SEM and laser scattering. The XRD only showed the partial dissociation of zircon and failed in the differentiation of its nanoconfigurations observed by PAC. The milling of this hard material can be optimized through the performed characterization strategy.

Graphical abstract

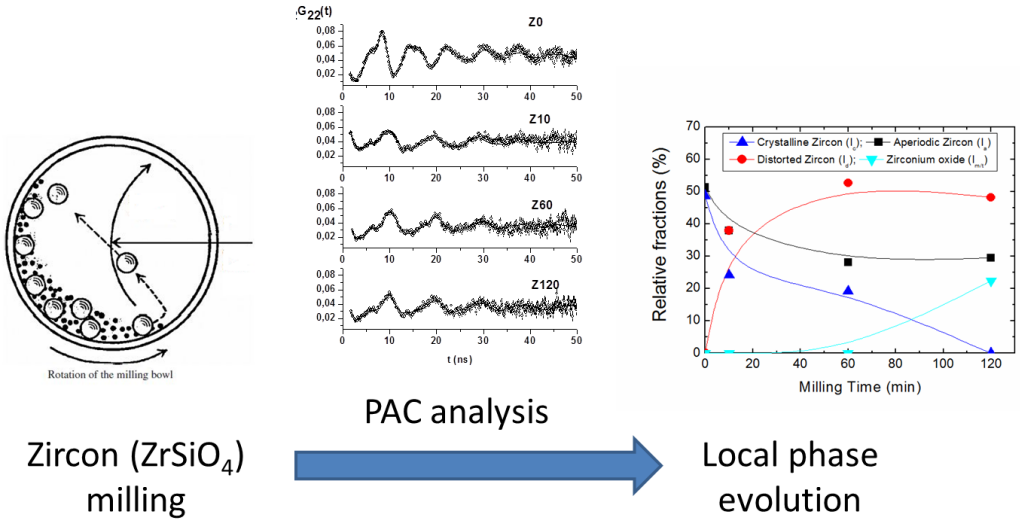

Key words: Zircon powder, milling, structure, perturbed angular correlations

1. Introduction

Zircon is an easily accessible mineral and is the main source for zirconium oxide, the metallic zirconium and other materials production [1-3]. Besides, zircon ceramics present interesting physical and chemical properties for technological use. Its main properties are: important hardness (7.5 Mohs), a moderately low linear thermal expansion (4.10^{-6} °C^{-1})

and a high dissociation temperature (1675 °C) [4-9]. It is also highly inert, even in contact with molten glass or slag. That is why it is used in applications at elevated temperatures (1300–1500 °C) with low chemical attack, as in the steel or glass industry [4] [10-12].

Its chemical stability makes zircon suitable for environmental barrier coatings in the chemical industry. For the same reason, it has been considered in the nuclear industry for high level waste disposal of actinides [13]. On the other hand, it possesses a high dielectric constant and a large energy gap, thus emerging as a high-κ gate dielectric material in the metal oxide-semiconductor technology [14].

The principal structural unit of zircon is a chain of alternating edge-sharing SiO_4 tetrahedra and ZrO_8 triangular dodecahedra extending parallel to the c-axis [4]. The chains are joined laterally by edge – sharing dodecahedra. The unit cell parameters are a= 6.6164 Å and c= 6.0150 Å [15]. Zircon is a highly stable structure, which decomposes at about 1670 °C to yield zirconia and silica. Due to their high melting point, high density sintered ceramics from pressed powders are difficult to achieve. Additives or their combination with other phases such as SiO_2, TiO_2, Al_2O_3, clays, etc. are commonly used to increase the final density and reduce porosity. However, these additions may be detrimental to mechanical properties such as hardness or fracture toughness. The mechano-chemical activation process using high energy milling has proved to be an effective technique as pretreatment of raw materials to obtain dense ceramics. The effect of the high energy milling is to activate chemical and physical processes due to the increase of the superficial energy and at the same time, yielding homogeneous mixtures [16-17].

The first attempt to study mechanical activation of zircon was by Motoi (1978). It was demonstrated that prolonged ball milling not only causes size reduction but also

amorphizes the mineral, leads to partial decomposition into ZrO_2 and SiO_2 and, can enhance solubility in HF [18].

Welham (1998, 2002) used ball milling up to 150 h to accomplish mechano-chemical reaction of zircon with alkaline earth metal oxides in order to form zirconia or zirconates, either within the mill or during subsequent annealing at 1200 °C [19-20]. About tenfold increase in hydrochloric acid solubility was observed when zircon was milled alone and milled with the oxides. Abdel-Rehim (2005) showed that almost complete recovery of zirconium from zircon was possible by simultaneous ball milling and alkaline leaching using sodium hydroxide (1.5 times the theoretical requirement) at 250 °C for 3 hours [21]. Attrition milling of zircon was used by Amer (2006) as a pretreatment to enhance alkaline pressure leaching of zircon; however, no attempt was made to characterize the activated solid except for the change in particle size [22].

The phenomenological effect of the mechanical milling of coarse zircon powder (150 µm) was recently assessed; the structural analysis consisted in the XRD experiment and posterior alkali leaching tests for pondering the non-stoichiometric dissolution of SiO_2 and ZrO_2 [23]. The milling conditions were more drastic than other previous studies but milder to the ones studied in the present work. Final particle size was between 1 and 2 µm for long term treatments 240 – 480 minutes. In that work, based on the rate constant values, it was found that the rate constant for the dissolution of ZrO_2 component is 1.6–5.0 folds higher than SiO_2 component depending upon mechanical activation time and leaching temperature. The prospect of the mechanical activation assisted alkali leaching of zircon is highlighted.

In a recent article we presented a systematic study of the effect of a high energy milling treatment in the subsequent direct sintering of fine zircon powder. The activated powders

sintered 200 °C below the un-milled powders [24]. The XRD permitted to identify the incipient partial dissociation of the zirconium silicate after long term (60-120 minutes) high energy milling treatments. This slight dissociation was also observed after the thermal treatments of the studied powders. The traditional XRD analysis failed to observe any structural changes in the zircon phase after these high energy milling treatments that evidently enhanced the posterior sintering behavior.

Details of the atomic arrangements of materials of technological uses were studied using short range methods as extended X-ray absorption fine structure (EXAFS) [25] and the perturbed angular correlations (PAC) techniques [26-27]. In particular, PAC technique has proved to be an efficient tool in the investigation of the milling effect of the monoclinic zirconia by showing the quadrupole interactions of special atomic arrays through which the monoclinic phase transforms into the tetragonal form [28-29].

The aim of the present work is to accurately identify and characterize the resulting phases during mechano-chemical activation process on fine zircon commercial powder ($D_{50}\cong 0.8$ µm). Perturbed Angular Correlations technique has been applied to investigate nanoconfigurations content in $ZrSiO_4$ as a function of milling time. The results will be discussed together with those obtained using XRD, SEM-EDS and laser scattering. The knowledge acquired will enlighten ceramic designers to improve ceramics properties and utilities; and other posterior industrial processing of this silicate.

2. Experimental procedure

2.1. Starting material

A commercial zircon fine powder (Kreutzonit Super Extra Weiß, Mahlwerke Helmut Kreutz GmbH, Germany, 0.8 μm) was used (Z0). Its chemical composition is (wt. %): ZrO_2:64–65.5, SiO_2:33–34, $Fe_2O_3 \leq 0.1$, $Al_2O_3 \leq 0.1$, $TiO_2 \leq 0.15$. The average particle size is D_{50}=0.8 mm, and it has a surface area of 4.1 m^2/g with a melting point of 2200 °C, and hardness of 7.5 Mohs. Its specific gravity is 4.5 g/cm^3.

The zircon (Z0) milling was carried out in planetary mill high energy ball milling (HEBM - 7 Premium Line, Fritsch Co., Ltd., Germany) in ethanol at 850 rpm. The treatment was performed for 10, 60 and 120 minutes, (Z10, Z60 and Z120, respectively). 85 mL magnesia stabilized zirconia jars were used with 60 g of zirconia balls (10 mm diameter) as milling media; the ratio between the weight of powder and the milling balls was 1:10 in each batch. The jars were naturally cooled down every 5 minutes.

2.2. Powder characterization

Milled zircon powders (Z10, Z60 and Z120) and original powder (Z0) were characterized by X-ray diffraction (XRD- Philips PW 3710 with Kα: Cu as incident radiation and Ni filter). The equipment was operated at 40 kV and 35 mA and the scanning was performed with a step of 0.04° and 2 seconds per step in the 2θ range between 10 and 80°. The particle shape and morphology were analyzed with scanning electron microscopy (SEM-JEOL JMS -6000, Japan). An EDS analysis was carried out as well. In order to observe the evolution of the particle size as a function of milling time, a Laser Diffraction Particle Size Distribution Analyzer (Malvern Hydro 2000G) was used.

To evaluate the effect of the milling treatment on zircon powders, a simple sintering process was carried out. A heating rate of 5 °C/min and a soaking time of 120 minutes

were employed, in an electric furnace in air atmosphere. The final temperature was 1500 °C. 1.0 gram and 15 mm diameter disc shape samples were prepared, first uniaxially pressed and then isostatically pressed at 1000 MPa. Apparent density and open porosity were evaluated as sintering parameters by the immersion method. A more systematic evaluation of the milling sintering relation has been previously published [24].

2.3. Perturbed Angular Correlation (PAC) analysis of the milled zircon ($ZrSiO_4$)

The Perturbed Angular Correlation (PAC) technique provides a nanoscopic (i.e. short-range) description of the crystalline lattice by determining the electric field gradients at Zr sites [30-31]. The nuclei of ^{181}Hf, obtained by irradiation with thermal neutrons, (RA3-reactor of the Comisión Nacional de Energía Atómica (CNEA)) of the ^{180}Hf natural impurities in Zr constitute the radioactive probes of the material. Briefly, the method consists in the examination of the angular correlation of the 133–482 keV γ- γ cascade emitted during the ^{181}Hf to ^{181}Ta β– decay. The probe nuclei report on the intensity (through the quadrupole frequency ω_Q), and the symmetry (through the asymmetry parameter:η) of the electric field gradient and its abundance or relative population f, if non-equivalent Zr sites occur. In addition, the degree of local disorder due to the presence of impurities or defects in lattice can be measured through the frequency distribution widths (δ). On account of the r^{-3} dependence of the quadrupole interaction, the technique is extremely localized and non-equivalent probe surroundings can be determined (f relative population). Theoretical functions of the form $A_{22}G_{22}(t)$, folded with the measured time resolution curve, were fitted to the experimental ratio R(t) to determine the magnitudes of interest. Measurements were performed at room

temperature using a four BaF_2-detector set up with high resolution (FWHM 0.6ns at Hf energies). Details on the experimental setup adopted in this work as well as fitting procedure can be found elsewhere [32].

3. Results and Discussion

The effect of the high energy ball milling (HEBM) pretreatment might result in partial zircon dissociation [4]:

$$\mathrm{ZrSiO_4} \leftrightarrow (\mathrm{m}-\mathrm{t})\ \mathrm{ZrO_2} + \mathrm{SiO_2(amorphous)} \qquad (1)$$

Figure 1 compares the XRD patterns of the powder before and after the HEBM. Regardless of the milling time, all the observed diffraction peaks belong to the zircon phase. No important broadening of the peaks is observed, apparently showing that the pretreatment did not affect the zircon crystallinity. This is expected due to the high hardness of the silicate (7.5 in the Mohs scale). The inset in this figure shows the main peaks of the zirconia phases (m and t/c) in the 2θ range. Only after 60 minutes of pretreatment a small band appears at 30.3 degrees, which corresponds to the high energy (tetragonal and/or cubic) zirconia phases [33]. After the 120-minute treatment, this peak is bigger but still small. It is accompanied by the main monoclinic (lower energy) zirconia peaks located at 28.3 ° and 31.5 °, corresponding to the (-111) and (111) planes. All this was clear evidence of the incipient silicate dissociation.

3.1. Milled powder particle size and morphology SEM and laser scattering analyses

Figure 2 shows SEM images of the Z0 and Z120 samples at two magnifications (x10000 and x30000). Figures 2a and 2c depict the SEM image of the as-received zircon powder, showing sharp edges and grain sizes between 0.1 µm and 2 µm. Figures 2b and 2d show the powder after 120 minutes of HEBM. After the milling process, the particles were more rounded, but no significant change in the particle size was detected, which was also observed by laser diffraction. No important agglomeration was observed, evidencing that the milling treatment affected grain morphology rather than particle size.

A global EDS analysis of the milled powder was carried out, (1000 seconds); the only detected elements were, as expected, zirconium and silicon. The milling media employed was magnesia stabilized zirconia. No magnesium was detected in the mentioned EDS test; hence, it can be stand that the milling treatments did not incorporate zirconia to the milled powder due to the jars or milling media.

Particle size distribution analysis was performed for the original (Z0) and the milled samples at 10, 60 and 120 minutes (Z10, Z60 and Z120, respectively) in order to observe the particle size evolution. Table 1 lists the results of the particle size analysis. The observed effect of the milling treatment is negligible. The mean particle size remained constant even after 120 minutes of pretreatment. These results are concordant with the SEM images in figure 2a-d.

3.2. Effect of the high energy milling treatment in zircon sintering.

The milling treatment of these hard powders, if it is enough energetic, might activate several processes like acid leaching, thermal decomposition and sintering. Figure 3 shows the sintering parameters of the milled fine zircon powders. Evidently, the sintering process was enhanced by the milling treatment. The as received powder resulted in 8% porosity after the proposed thermal treatment; even short time treatment enhanced the sinterization. No porosity, negligible within the performed Archimedes method accuracy, was detected in the 60 and 120 minutes milled powders. The achieved density of the materials after the heating treatment (1500 °C) was increased by the milling pretreatment. This is an experimental evidence of the structural changes during the milling treatment. These were difficult to observe in the XRD patterns, SEM and particle size distribution characterizations. All these evidence that the structural changes are subtle and consists in local distorted structural changes in the zircon structure. The PAC characterization arises as an adequate strategy for evaluating the milling effect in these hard powder materials.

4. Effect of the high energy milling treatment in zircon, perturbed angular correlation (PAC) analysis.

Figure 4 shows the spin rotation curves obtained from PAC experiments of the as-adquired and milled powders.

For the as-received zircon (Z0), a two-site hyperfine pattern had to be assumed to achieve a satisfactory fit. These two components are the well-known interaction describing crystalline zircon [6] hereinafter named I_c and a second one, I_a related to an aperiodic zircon highly asymmetric and distributed.

As milling time proceeds, the hyperfine pattern changed requiring three components to well describe the whole pattern.

As a consequence of the first 10 minutes of milling it is observed the appearance of the relative fraction of a distorted (I_d) $ZrSiO_4$ at expenses of that of the crystalline zircon that remains until the last milling step. This interaction has a similar quadrupole frequency to crystalline zircon with a high asymmetry parameter and wide spread, reflecting a significant local disorder [30]. This combination of three contributions I_c, I_a and I_d persist up to 60 minutes of milling. Incorporating zirconium oxide phases did not improved the fitting results for Z60. It is worthy to note, that this feature is consistent with XRD analysis, since these three contributions describe different surroundings of Zr atoms in zirconium silicates ($ZrSiO_4$).

In addition, the quadrupole frequency mean value for I_a varies with milling time from 83 for Z0 to 66 Mrad/s for the rest of the treatments, which is clearly appreciated in figure 4.

After the last milling step (120 minutes) a new widely distributed hyperfine interaction appears which can be assigned to m/t-ZrO_2. This new compound indicates that the decomposition of zircon has begun, at expenses of crystalline zircon. The m/t-ZrO_2 phase was already reported by Scian et al. [25] when milling pure Zirconia, in similar experimental conditions. This fact is in agreement with the appearance of m/t-ZrO_2 diffraction peaks observed by XRD (fig. 1). However, the great amount of m/t ZrO_2 observed by PAC is probably due to the high local character of this nuclear technique.

In table 2, the quadrupole parameters determined via the fitting procedure are listed together with references values for comparison.

Figure 5 shows the milling time evolution of relative fractions corresponding to each quadrupole interactions. It is important to note that PAC technique only probes Zr containing compounds.

Taking into account the observed evolution of the relative fractions determined by PAC (see figure 2) we can suggest the following sequence of reactions:

$$\boldsymbol{ZrSiO_4(c) \leftrightarrow ZrSiO_4(a)} \quad (2)$$

$$\boldsymbol{ZrSiO_4(a) \leftrightarrow ZrSiO_4(d)} \quad (3)$$

Any of these three zircon phases (c, a, d) can dissociate into a zirconia and a silicon oxide phase [25].

$$\boldsymbol{ZrSiO_4(x) \leftrightarrow ZrO_2(d) + SiO_2} \quad (4)$$

However, our PAC results suggested that it is the crystalline structure which gives rise to the m/t ZrO_2.

By considering the results of XRD and PAC, the effects of milling on the fine zircon we can determine: The HEBM treatment did not modify notoriously the particle size of fine zircon, but its morphology changed, as can be observed in particle size distribution data (table 1) and in SEM images (Figure 2). By XRD, the main phase identified throughout the milling time range was zirconium silicate. There were no major changes except mild widening of the peaks and the incipient dissociation of silicate, evidenced by the appearance of peaks belonging to tetragonal and monoclinic zirconia.

PAC analysis, being a very local technique, identified two equally populated sites in the original fine zircon corresponding to crystalline zircon and aperiodic zircon. As milling proceeds, many defects are introduced which give rise to a new interaction reflecting highly disordered sites.

Thus, a transition from the more ordered zircon phases to lower ordered ones depending on the processing variable is clearly observed.

In agreement with XRD results, after long milling times, PAC reported the presence of zirconium oxide. However, it is important to point out that the relative amount of zirconium oxide evaluated is higher than the amount of zirconia inferred by XRD. This could be explained by the low crystalline nature of the zirconium oxide produced by the milling treatment and to the different capabilities of the employed technique.

Finally, it can be stand that the partial dissociation resulting in the appearance of zirconium oxide and amorphous silica will undoubtedly affect and, due to the second, enhance the sintering of this hard and refractory powder.

5. Conclusions

The milling effect of a hard mineral powder ($ZrSiO_4$) was assessed by means of complimentary techniques. The phenomenological macroscopic confirmation of the structural change and mechanical activation consisted in the important enhancement of the sintering behavior of the treated fine zircon powders; presumably other post treatments like chemical leaching might be enhanced as well.

No important change in the particle size distribution was observed, only a slight morphological change was detected by SEM. The XRD showed only the partial

dissociation and failed in the differentiation of the zircon nano-configurations observed by PAC. By means of this technique, three different well known zircon phases were identified and quantified as a function of the milling time: a fully crystalline phase, an aperiodic phase and a distorted one, coming from the first two phases.

With long term treatments a partial dissociation was observed, yielding a zirconium oxide highly distorted. The formed corresponding silica enhances the sintering of this hard and refractory fine powder.

Finally, it is worth to point out that the processing conditions of this material can be optimized through the performed characterization strategy.

References

[1]. L. Yin, Y. Xu, Z. Huang, Y. Liu, M. Fang, B. Liu, Synthesis of ZrN–Si3N4 composite powders from zircon and quartz by carbothermal reduction and nitridation, Powder Technol. 246 (2013) 677-681. ISSN 0032-5910, http://dx.doi.org/10.1016/j.powtec.2013.06.029.

[2]. P. Manivasakan, A. Karthik, V. Rajendran, Mass production of Al2O3 and ZrO2 nanoparticles by hot-air spray pyrolysis, Powder Technol. 234 (2013) 84-90. ISSN 0032-5910, http://dx.doi.org/10.1016/j.powtec.2012.08.028.

[3]. S. Srikanth, V. L. Devi, R. Kumar, Unfolding the complexities of mechanical activation assisted alkali leaching of zircon ($ZrSiO_4$), Hydrometall. 165 (2016) 125-136.

[4]. A. Kaiser, M. Lobert, R. Telle, Thermal stability of zircon (ZrSiO4), J. Eur. Ceram. Soc. 28, 11, (2008) 2199-2211. ISSN 0955-2219, http://dx.doi.org/10.1016/j.jeurceramsoc.2007.12.040.

[5]. X. Carbonneau, M. Hamidouche, C. Olagnon, G. Fantozzi, R. Torrecillas, High temperature behaviour of a zircon ceramic. Key Eng. Mater. 132 (1997) 571-574.

[6]. N.M. Rendtorff, G. Suárez, Y. Sakka, E.F. Aglietti, Dense mullite zirconia composites obtained from the reaction sintering of milled stoichiometric alumina zircon mixtures by SPS, Ceram. Int. 40, 3 (2014) 4461-4470.

[7]. N.M. Rendtorff, S. Grasso, C. Hu, G. Suarez, E.F. Aglietti, Y. Sakka, Zircon-zirconia ($ZrSiO_4$-ZrO_2) dense ceramic composites by spark plasma sintering, J. Eur. Ceram. Soc. 32, 4(2012) 787-793.

[8]. N.M. Rendtorff, S. Grasso, C. Hu, G. Suarez, E.F. Aglietti, Y. Sakka, Dense zircon ($ZrSiO_4$) ceramics by high energy ball milling and spark plasma sintering, Ceram. Int. 38, 3 (2012) 1793-1799.

[9]. G. Suárez, S. Acevedo, N.M. Rendtorff, L.B. Garrido, E.F. Aglietti, Colloidal processing, sintering and mechanical properties of zircon ($ZrSiO_4$), Ceram. Int. 41, 1 (2015) 1015-1021.

[10]. M. Toshiyuki, Y. Hiroshi, K. Hidehiko, M. Takashi, Sintering of high purity ZrSiO4 powder, J. Ceram. Soc. Jpn. 99, 11 (1991) 1058.

[11]. M. Toshiyuki, H. Hirokuni, Y. Hiroshi, K. Hidehiko, M. Takashi, Mechanical properties of high purity sintered $ZrSiO_4$, Nippon Seramikkusu Kyokai Gakujutsu Ronbunshi/J. Ceram. Soc. Jpn. 98, 9 (1990) 1017-1022.

[12]. J. S. Lee, J. B. Kang, Sintering Characteristics of Zircon Nanopowders Fabricated by High Energy Milling Process, Korean J. Mater. Res. 26, 2 (2016) 95-99.

[13]. R. C. Ewing, W. Lutze, W. J. Weber, Zircon: A host-phase for the disposal of weapons plutonium, J. Mater. Res. 10, 2 (1995) 243-246.

[14]. G. D. Wilk, R. M. Wallace, J. M. Anthony, High-κ gate dielectrics: Current status and materials properties considerations. J. Appl. Phys, 89, 10 (2001) 5243-5275.

[15]. R. E. Alonso, L. Errico, M. Taylor, A. Svane, N. E. Christensen, Structural, electronic and hyperfine characterization of pure and Ta-doped ZrSiO4, Phys. Rev. B, 91, 8 (2015) 085129.

[16]. C. Suryanarayana, Mechanical alloying and milling, Prog. Mater. Sci. 46, 1-2, (2001) 1-184.

[17]. V. N. Antsiferov, V.B. Kul'met'eva, S.E. Porozova, B.L. Krasnyi, V.P. Tarasovskii, A.B. Krasnyi, Application of mechanochemical activation in production of zircon ceramics, Rus. J. Non-Ferr. Met. 51, 2 (2010) 182-187.

[18]. S. Motoi, Mechanochemical effect in zircon by mechanical grinding, J. Ceram. Assoc. Jpn. 86, 990, (1978) 92–95.

[19]. N. J. WELHAM, Investigation of mechanochemical reactions between zircon ($ZrSiO_4$) and alkaline earth metal oxides. Metall. Mater. Trans. B. 29, 3, (1998) 603-610.

[20]. N. J.WELHAM, New route for the extraction of crude zirconia from zircon. J. Am. Ceram. Soc. 85, 9, (2002) 2217-2221.

[21]. A. M. ABDEL-REHIM, A new technique for extracting zirconium form Egyptian zircon concentrate, Int. J. Miner. Proc. 76, 4, (2005) 234-243.

[22]. M. A. ASHRAF, Kinetics of alkaline pressure leaching of mechanically modified zircon concentrate, Phys. Prob. Miner. Proc.40 (2006) 61-68.

[23]. S. Srikanth, V. L. Devi, R. Kumar, Unfolding the complexities of mechanical activation assisted alkali leaching of zircon (ZrSiO4), Hydrometall. 157(2015) 159-170.

[24]. M. Gauna, G. Suárez, M.S. Conconi, E.F Aglietti, N.M. Rendtorff, Dense zircon ($ZrSiO_4$) ceramics by a simple milling-sintering route. (Sci. Sinter., In press, Accepted for publication 2017).

[25]. F. Farges, The structure of metamict zircon: A temperature-dependent EXAFS study, Phys. Chem. Miner. 20, 7, (1994) 504-514.

[26]. H. Jaeger, L. Abu-Raddad, D. J. Wick, TDPAC study of structural disorder in metamict zircon, Appl. Radiat. Isot. 48, 8, (1997) 1083-1089.

[27]. N.M. Rendtorff, M.S. Conconi, E.F. Aglietti, C.Y. Chain, A.F. Pasquevich, P.C. Rivas, J.A. Martínez, M.C. Caracoche, Phase quantification of mullite-zirconia and zircon commercial powders using PAC and XRD techniques, Hyperfine Interact., 198, 1, (2010) 211-218.

[28]. A. N. Scian, E. F. Aglietti, M. C. Caracoche, P. C. Rivas, A. F. Pasquevich, A. R. Lopez Garcia, Phase transformations in monoclinic Zirconia caused by milling and subsequent annealing, J. Amer. Ceram. Soc. 77, 6, (1994)1525-1530.

[29]. N.M. Rendtorff, G. Suárez, E.F. Aglietti, P.C. Rivas, J.A. Martinez, Phase evolution in the mechanochemical synthesis of stabilized nanocrystalline (ZrO2)0.97(Y2O3)0.03 solid solution by PAC technique, Ceram. Int. 39, 5, (2013) 5577-5583.

[30]. H. Frauenfelder, R. M. Steffen, Angular correlation, Alpha-, Beta- and Gamma-Ray Spectrosc. 2 (1965) 997.

[31]. R. Dogra, A.P. Byrne, M.C. Ridgway, The Potential of the Perturbed Angular Correlation Technique in Characterizing Semiconductors, J. Electr. Mat. 38 (2009) 623-634.

[32]. L. Rubio-Puzzo, M.C Caracoche, M.M. Cervera, P.C. Rivas, A.M. Ferrari, F. Bondioli, Hyperfine Characterization of pure and doped zircons, J. Solid State Chem. 150 (2000) 14-18.

[33]. X. Jin, Martensitic transformation in zirconia containing ceramics and its applications, Curr. Opin. Solid State Mater. Sci.9, 6, (2005) 313, C318.

Figure 1: XRD patterns of the milled and un-milled fine zircon ($ZrSiO_4$) powders.

Figure 2: SEM images of the as-received and milled powders; a: Z0, x 10000; b: Z120, x10000; c: Z0, x30000; and d: Z120, x30000.

Figure 3: Sintering parameters: apparent density and open porosity of the sintered powders heated at 1500 °C as a function of milling time.

Figure 4: Spin rotation curves determined for the zircon powders. Full lines represent the fitting results.

Figure 5: Evolution of relative fraction with milling time.

Table 1: Particle size distribution of the milled zircon powders.

Sample	Milling time (min)	D_{10} (µm)	D_{50} (µm)	D_{90} (µm)
Z0	0	0.5	1.1	2.6
Z10	10	0.5	1.1	2.4
Z60	60	0.5	1.1	2.7
Z120	120	0.4	1.1	2.8

Table 2: Fitted quadrupole parameters: quadrupole frequency, ω_Q (Mrad/s); asymmetry parameter, η and frequency distribution δ (%), for each of the following contributions, crystalline zircon (I_c); aperiodic zircon (I_a); distorted zircon (I_d) and monoclinic/tetragonal zirconia ($I_{m/t}$). Also references values are displayed.

Parameter	Interactions				References			
	I_c	I_a	I_d	$I_{m/t}$	Crystalline [32]	Aperiodic [26]	Distorted [32]	Monoclinic/tetragonal [28]
Chemical formula	$ZrSiO_4$	$ZrSiO_4$	$ZrSiO_4$	ZrO_2	$ZrSiO_4$	$ZrSiO_4$	$ZrSiO_4$	ZrO_2
ω_Q (Mrad/s)	106_1	66_1	98_3	155_1	100_1	85_1	100_2	165_5
η	0.19_2	0.83_1	1_1	0.5_1	0.21_1	0.74_1	0.98_3	0.48_2
δ (%)	2_1	6_1	29_7	15_1	10_1	15_1	1	3

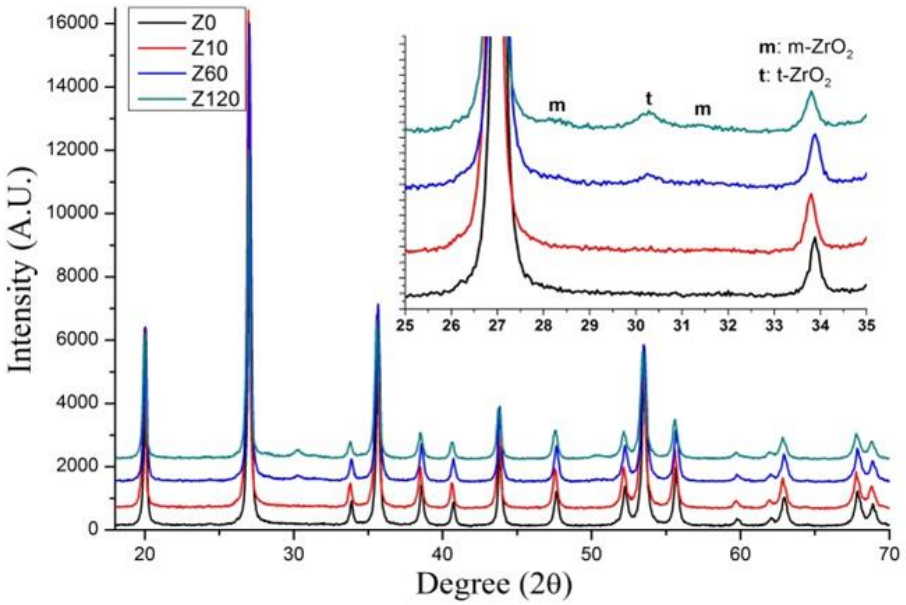
Z0
Z10
Z60
Z120
m: m-ZrO2
t: t-ZrO2
m
t
m
Intensity (A.U.)
Degree (2θ)

fig 1

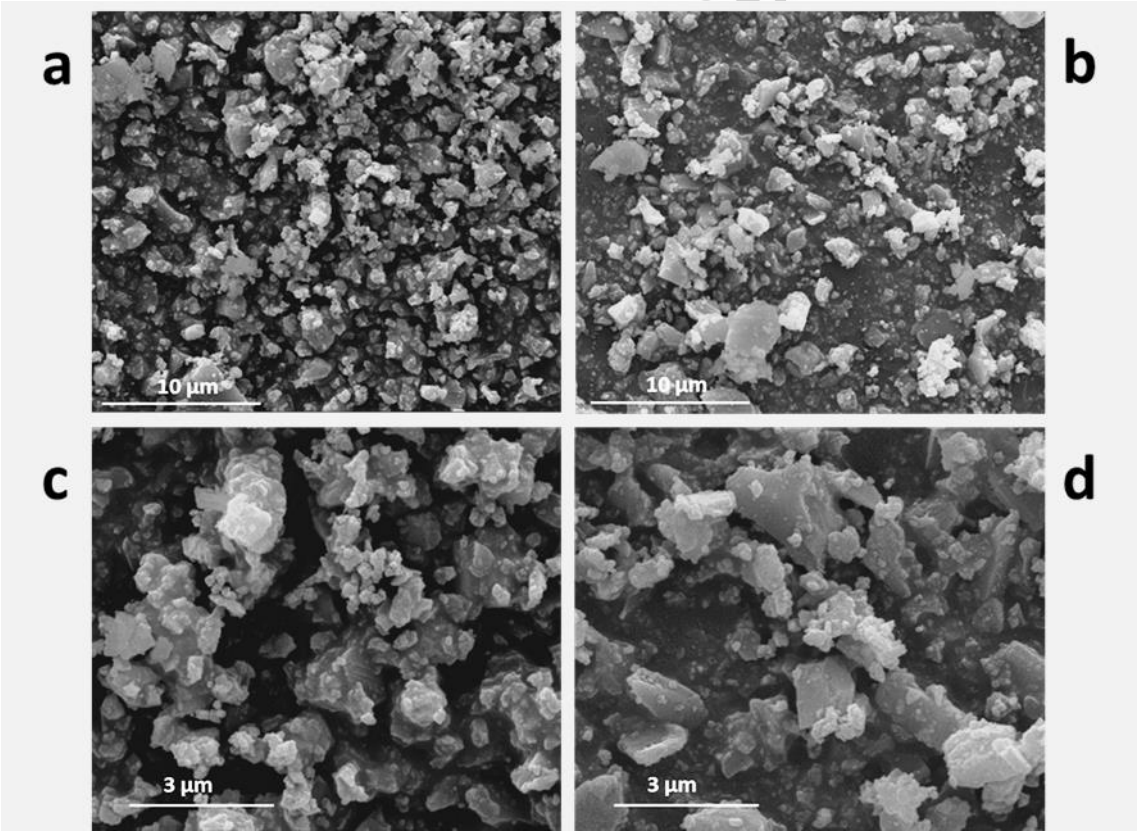
a
b
c
d
10 µm
10 µm
3 µm
3 µm

fig 2

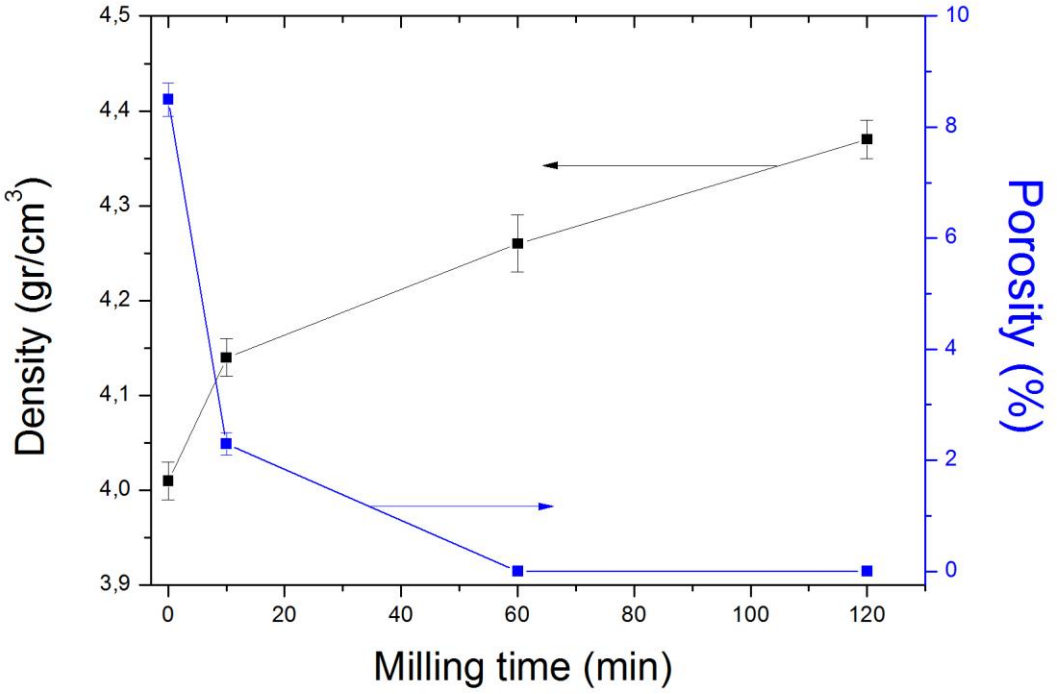

fig 3

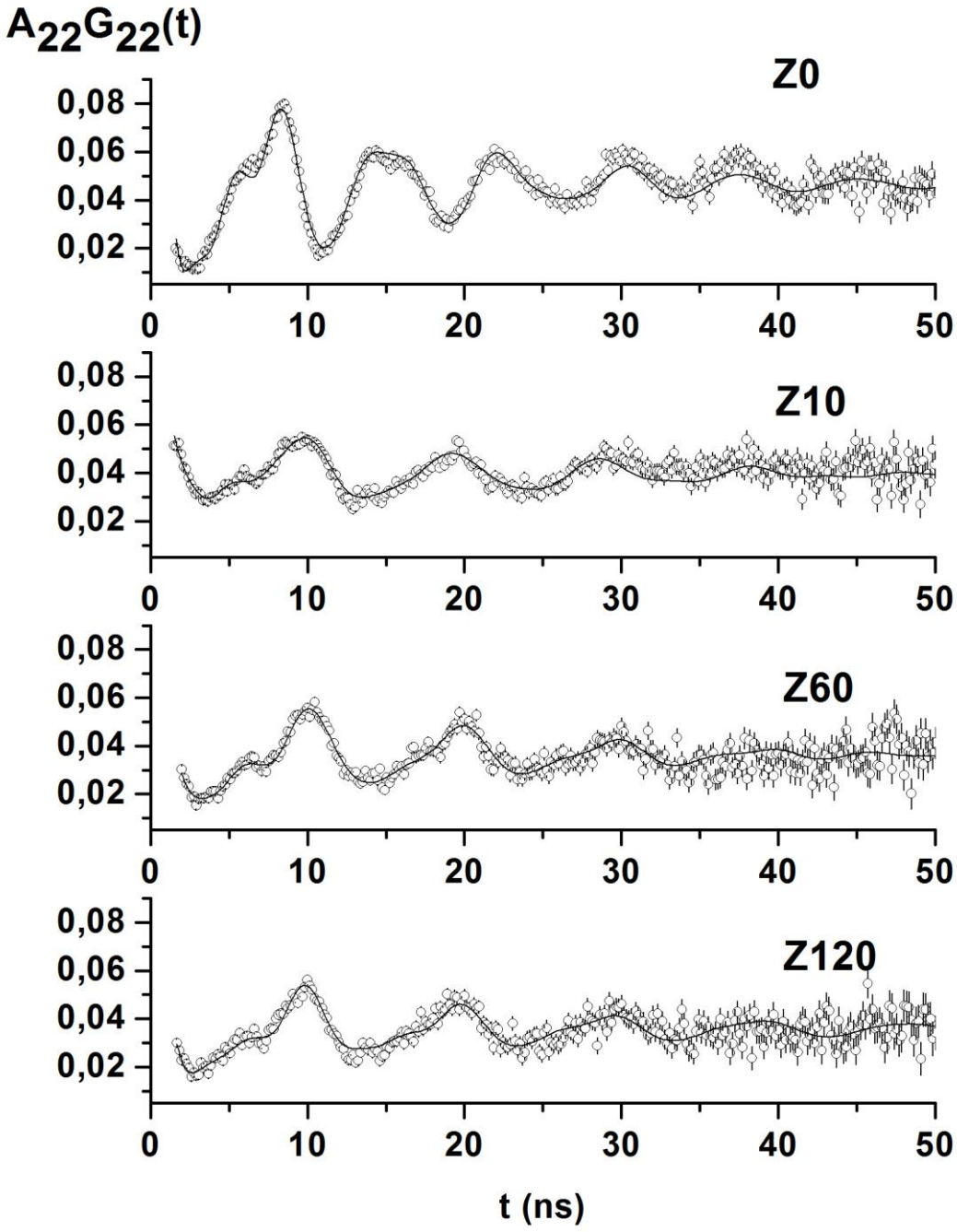

fig 4

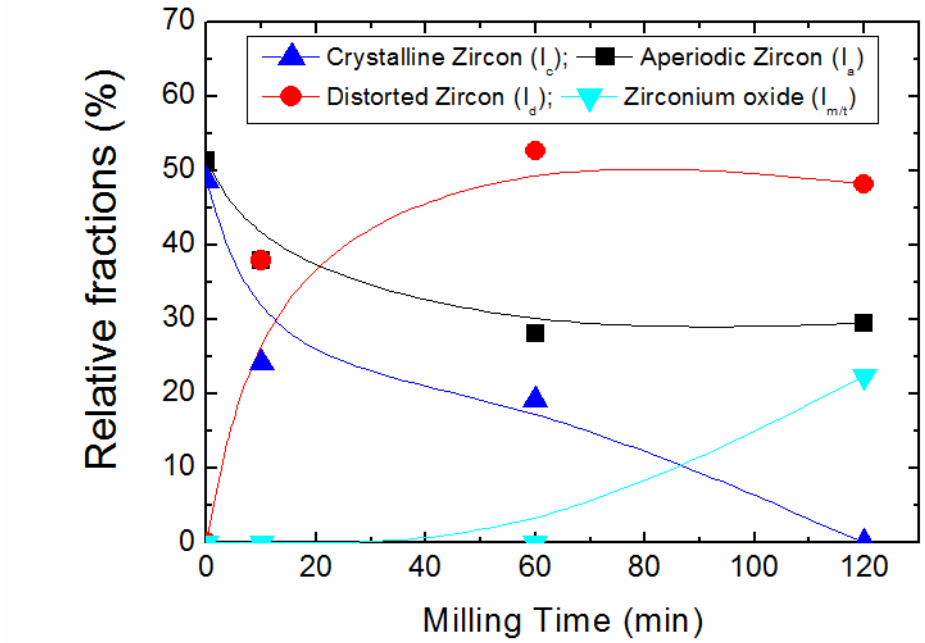

fig 5